Acta Pharmaceutica Sinica B 2025;15(4):2156−2169

Chinese Pharmaceutical Association
Institute of Materia Medica, Chinese Academy of Medical Sciences

Acta Pharmaceutica Sinica B

www.elsevier.com/locate/apsb
www.sciencedirect.com

ORIGINAL ARTICLE

GPC3-mediated lysosome-targeting chimeras (GLTACs) for targeted degradation of membrane proteins

Yuxin Fang[a,†], Yaojin Zhu[b,†], Wei Wang[a], Zhewei Xia[a], Shipeng He[b,*], Guoqiang Dong[a,*], Chunquan Sheng[a,*]

[a]*Center for Basic Research and Innovation of Medicine and Pharmacy (MOE), School of Pharmacy, Second Military Medical University (Naval Medical University), Shanghai 200433, China*
[b]*Institute of Translational Medicine, Shanghai University, Shanghai 200444, China*

Received 25 July 2024; received in revised form 23 September 2024; accepted 20 October 2024

KEY WORDS

Glypican-3;
PD-L1;
Lysosomal degradation;
Membrane protein;
Targeted protein degradation

Abstract Membrane protein degradation is a cutting-edge field in targeted protein degradation (TPD). Herein, we developed glypican-3 (GPC3)-mediated lysosome-targeting chimeras (GLTACs) as a novel strategy for the targeted degradation of tumor-specific membrane proteins. GLTACs utilize tumor-specific expression and endocytosis properties of GPC3 to degrade membrane proteins. By conjugating a GPC3-targeting peptide with the ligand of protein of interest (POI), GLTACs induce the formation of a ternary complex that is internalized into lysosomes, leading to the degradation of the POI. The effectiveness and specificity of GLTACs were validated by designing PD-L1, c-Met, and FGFR1 degraders. In particular, GLTAC **WP0** potently degraded PD-L1 and induced T-cell-mediated tumor killing against HepG2 cells, highlighting the potential therapeutic applications. The development of GLTAC technology expands the scope of TPD strategies and opens new avenues for discovering novel therapeutic modalities against challenging protein targets.

*Corresponding authors.
E-mail addresses: heshipeng@shu.edu.cn (Shipeng He), gdong@smmu.edu.cn (Guoqiang Dong), shengcq@smmu.edu.cn (Chunquan Sheng).
[†]These authors made equal contributions to this work.
Peer review under the responsibility of Chinese Pharmaceutical Association and Institute of Materia Medica, Chinese Academy of Medical Sciences.

https://doi.org/10.1016/j.apsb.2025.02.037

1. Introduction

Targeted protein degradation (TPD) technology has emerged as a hotspot in drug development over the past two decades[1]. By harnessing the natural degradation system in cells to eliminate disease-related proteins, TPD has demonstrated significant advantages in overcoming drug resistance and targeting undruggable proteins[2,3]. Among various TPD technologies, proteolysis targeting chimeras (PROTACs) have gained considerable attention, with several drug candidates entering clinical research trials[4]. PROTAC molecules, consisting of E3 ligase ligands, protein of interest (POI) binders, and linkers, recruit E3 ligases in an event-driven manner to induce ubiquitination and proteasomal degradation of the POIs[5]. However, due to reliance on the ubiquitin-proteasome system, PROTAC technology faces limitations in degrading membrane proteins[6].

Extracellular and membrane-associated proteins account for approximately 40% of human genome-encoded proteins and represent an important family of drug targets[7]. Membrane proteins play key roles in various biological processes and are closely associated with the development of diseases such as cancer, aging, metabolic disorders, and immunological diseases, making them the targets for more than half of the known drugs[8]. Therefore, developing novel strategies for eliminating membrane proteins not only expands the application scope of TPD technologies but also holds promising value for drug development[8]. Current degradation strategies for extracellular and membrane proteins mainly include lysosome-targeting chimeras (LYTACs)[9], cytokine receptor-targeting chimeras (KineTACs)[10], dendronized DNA chimera (DENTAC)[11], and integrin-facilitated lysosomal degradation (IFLD)[12]. LYTAC represents the pioneering technology for degrading extracellular and membrane proteins, wherein lysosome-targeting receptors and POIs are connected *via* antibody conjugates to form ternary complexes[9]. The complexes are internalized through lysosome-targeting receptors and subsequently transported to lysosomes for POIs degradation. LYTAC primarily utilizes two lysosome-targeting receptors: the cation-independent mannose-6-phosphate receptor (CI-M6PR) and the liver-specific asialoglycoprotein receptor (ASGPR)[13]. Additionally, there are other membrane protein degradation approaches such as covalent nanobody-based PROTAC strategy (GlueTAC), bispecific aptamer chimeras, and antibody-based PROTAC (AbTAC) that recruit the membrane-bound E3 ubiquitin ligases (*e.g.*, RNF43)[14-16].

Despite these progresses, the development of membrane protein degradation technologies still faces huge challenges. Firstly, most degradation strategies rely on large biomolecules (such as bispecific antibodies, aptamers, etc.), which are generally limited by complex molecular structures, synthetic difficulty, and poor stability. Secondly, antibodies and oligosaccharide ligands used in LYTAC may exhibit immunogenicity, and there is uncertainty in the drug-to-antibody ratio and the connection sites of antibody conjugates[17]. In addition, CI-M6PR is widely expressed in cells and liver tissue-specific ASGPR is also prevalent in normal liver cells. Overactivation of these lysosomal-targeting receptors for internalization may affect their normal physiological functions, resulting in potential toxic side effects and acquired drug resistance. Therefore, exploring lysosome-targeting receptors with tumor specificity and developing new membrane protein degradation technologies with simple molecular structures and synthetic convenience is highly desirable.

Heparan sulfate proteoglycans (HSPG) are a class of classic cell-surface receptors responsible for the endocytosis of diverse macromolecular cargos[18]. Among them, Glypican-3 (GPC3) has gained much attention due to its close association with the occurrence and development of cancer[19]. GPC3 is overexpressed in more than 70% of patients with hepatocellular carcinoma (HCC), while it is nearly absent in normal adult liver tissue[20]. This high specificity makes GPC3 a potential target for HCC diagnosis and treatment[21]. Furthermore, GPC3 can negatively regulate signal activation by continuously removing Hedgehog from the cell surface through endocytosis and transporting it to lysosomes for elimination[22]. Previously, we have confirmed that GPC3-mediated endocytosis promotes the internalization of GPC3-targeting photosensitizer into HepG2 liver cancer cells and enriches them in lysosomes[23]. Considering the endocytosis properties of GPC3 and its specificity expression in HCC and other cancer cells, we envisioned that GPC3 was an ideal lysosomal-targeting receptor for membrane protein degradation.

Herein, we developed an innovative lysosomal degradation strategy, termed GPC3-mediated lysosome-targeting chimera (GLTAC). As illustrated in Fig. 1A, GLTAC is a bifunctional molecule composed of a GPC3-targeting ligand, a POI binding ligand, and an appropriate linker that connects them. GLTAC can induce the formation of a GPC3-GLTAC-POI ternary complex, thereby promoting endocytosis and subsequent lysosomal degradation of membrane POI. By utilizing the tumor-specific expression of GPC3, GLTACs have the capacity to selectively degrade membrane proteins in cancer cells. As a proof-of-concept study, we demonstrated that GLTACs can effectively induce the internalization and lysosomal degradation of several pathogenesis-related membrane proteins (*e.g.*, PD-L1, c-Met, and FGFR1) in GPC3-positive tumor cells. This research highlights the potential of GLTAC technology to address the limitations of current TPD strategies and offers a new strategy for the treatment of diseases characterized by the dysregulation of membrane proteins.

2. Results and discussion

2.1. Validation of GPC3-mediated endocytosis and lysosomal trafficking

Compound **8b** is a GPC3-targeting photosensitizer reported in our previous study (Fig. 2A)[23], which was designed by conjugating the GPC3-targeting peptide **TJ12P1** with the photosensitizer chlorin e6, aiming to achieve targeted photodynamic therapy for liver cancer. Herein compound **8b** was used as a fluorescent probe to evaluate the GPC3-mediated endocytosis in HepG2 HCC cells. Initially, we confirmed the high expression of GPC3 in HepG2 cells through flow cytometry analysis and Western blot experiments (Fig. 2B, Supporting Information Figs. S1 and S19). Subsequently, fluorescence confocal experiments showed that compound **8b** could enter into HepG2 cells and accumulate in lysosomes (Fig. 2C). Pretreatment of HepG2 cells with sodium heparin (a competitive inhibitor of HSPG) significantly inhibited the internalization of compound **8b**, indicating that the endocytosis of compound **8b** is GPC3-dependent. After incubation of HepG2 cells with compound **8b** for 24 h, colocalization of compound **8b** with lysosomes was observed using a lysosomal fluorescent probe (Fig. 2D). 3D fluorescence confocal imaging further confirmed the accumulation of compound **8b** in lysosomes (Fig. 2E). These findings collectively suggest that GPC3-targeting cargos enter the cells through GPC3-mediated endocytosis and are subsequently transported to lysosomes.

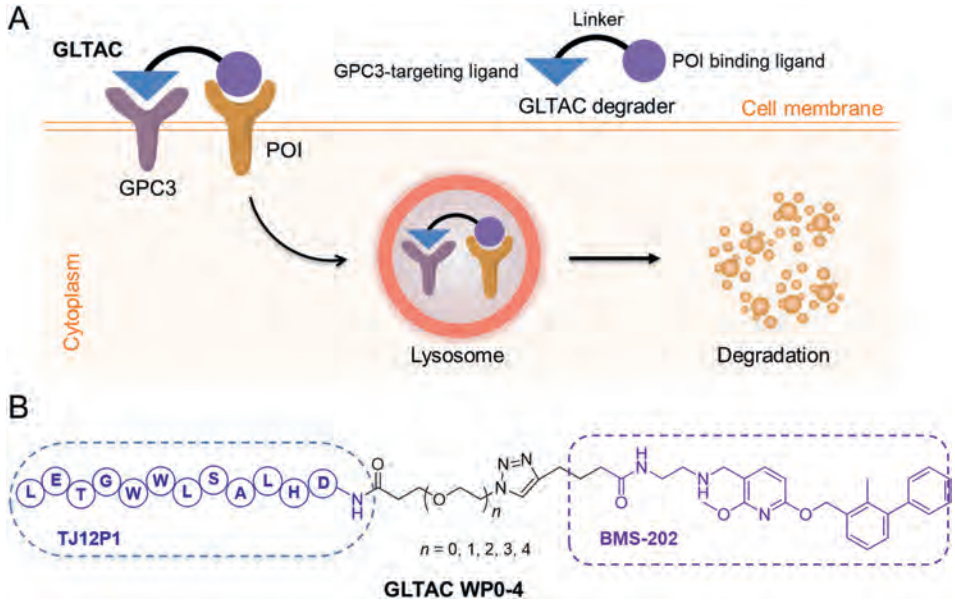

Figure 1 The GLTAC strategy for targeted membrane protein degradation. (A) The GLTAC molecule, consisting of a GPC3-targeting ligand, a POI-binding ligand, and a linker, hijacks the GPC3 receptor to induce the internalization and lysosomal degradation of POI. (B) Chemical structure of PD-L1 GLTACs.

2.2. Rational design and synthesis of PD-L1 GLTAC degraders

GLTACs are able to "hijack" the endocytosis of GPC3 to recruit membrane proteins for lysosomal degradation. To validate the feasibility of the GLTAC strategy, a proof-of-concept study was performed using immune checkpoint PD-L1 as the POI. PD-L1 is a classic target for tumor immunotherapy, which achieves tumor immune escape by interacting with PD-1[27]. **BMS-202** is a well-known small molecule inhibitor of PD-L1, which blocks the interaction between PD-1 and PD-L1, activates the immune system, and exerts antitumor effects[28]. Recently, **BMS-202-**based PROTACs have been reported. Among them, compound **PA8** exhibited potent PD-L1 degradation activity in 4T1 cells (DC_{50} = 0.609 μmol/L), providing a solid foundation for further research on PD-L1 degraders[29]. However, other PROTACs generally demonstrated poor PD-L1 degrading efficiency[30-32]. Based on the GLTAC design rationale, we designed a series of bifunctional GLTAC degraders by conjugating GPC3-targeting peptide **TJ12P1** and the PD-L1 inhibitor **BMS-202** through 1,2,3-triazole linkers (Fig. 1B).

The synthetic route of GLTACs **WP0-4** is outlined in Scheme 1 and Supporting Information Scheme S1. Initially, commercially available starting material **1** was reacted with 6-chloro-2-methoxynicotinaldehyde (**2**) to afford intermediate **3**. The key intermediate **4** was prepared according to the literature methods[31,32]. Subsequently, intermediates **3** and **4** underwent a reductive amination reaction to afford intermediate **5**. The GPC3-targeting peptide **TJ12P1** (DHLASLWWGTEL) was synthesized using the standard fluorenylmethyloxycarbonyl (Fmoc) solid-phase peptide synthesis (SPPS) method[23], employing 2-chlorotrityl chloride resin as the solid support. The deprotected resin was coupled with Fmoc-amino acids in anhydrous DMF at 30 °C for 1 h using HOBT and DIC as the coupling agents. The completion of the coupling step was confirmed by the ninhydrin method. After the reaction was complete, 20% piperidine DMF solution (*v*/*v*) was used to remove the Fmoc protecting groups. The polypeptide sequence (DHLASLWWGTEL) was assembled by linking each amino acid in turn. After coupling the final amino acid (Asp) to the resin, intermediate **6** was obtained. Then, using HATU and DIPEA as coupling agents, compounds azido-PEG_n-acids (n = 0, 1, 2, 3, 4) were reacted with intermediate **6** to obtain intermediates **7a**−**e.** To cleave intermediates **7a**−**e** from the resin, a mixture of TFA, TIPS, and H_2O (95% TFA, 2.5% TIPS, and 2.5% H_2O) was treated with intermediates **7a**−**e** for 1 h to give intermediates **8a**−**e**. Finally, using convenient click reactions, compounds **8a**−**e** reacted with compound **5** for 5 h at room temperature in the presence of $CuSO_4$ and sodium ascorbate to yield target compounds **WP0-4**.

2.3. Degradation of PD-L1 via GLTACs

HepG2 cells that simultaneously express GPC3 and PD-L1 were used to evaluate the degradation activities of the target compounds. The expression level of PD-L1 in HepG2 cells was confirmed by flow cytometry assay (Supporting Information Fig. S2). PD-L1 degradation was observed in all tested compounds at a concentration of 10 μmol/L, which preliminarily proved the feasibility of the GLTAC strategy (Fig. 3A, Supporting Information Figs. S3, S10 and S20). Structure−activity relationship (SAR) analysis revealed that the linker length significantly affected the degradation activity of GLTACs. GLTAC **WP0** with the shortest linker (eight atoms) showed the best PD-L1 degradation activity with a DC_{50} value of 0.38 μmol/L and a D_{max} value of 83% (Fig. 3A, Supporting Information Fig. S4). In addition, GLTAC **WP0** induced less PD-L1 degradation at a high concentration of 10 μmol/L compared to 3.3 μmol/L, indicating the presence of a hook effect. The GLTAC molecule with a relatively longer linker (**WP1**), also showed PD-L1 degradation activity (DC_{50} = 2.03 ± 0.38 μmol/L), whereas the activity was significantly lower than that of compound **WP0**. As the linker length was further increased, the DC_{50} values of the compounds all exceeded 3.3 μmol/L. Then, further visualization and

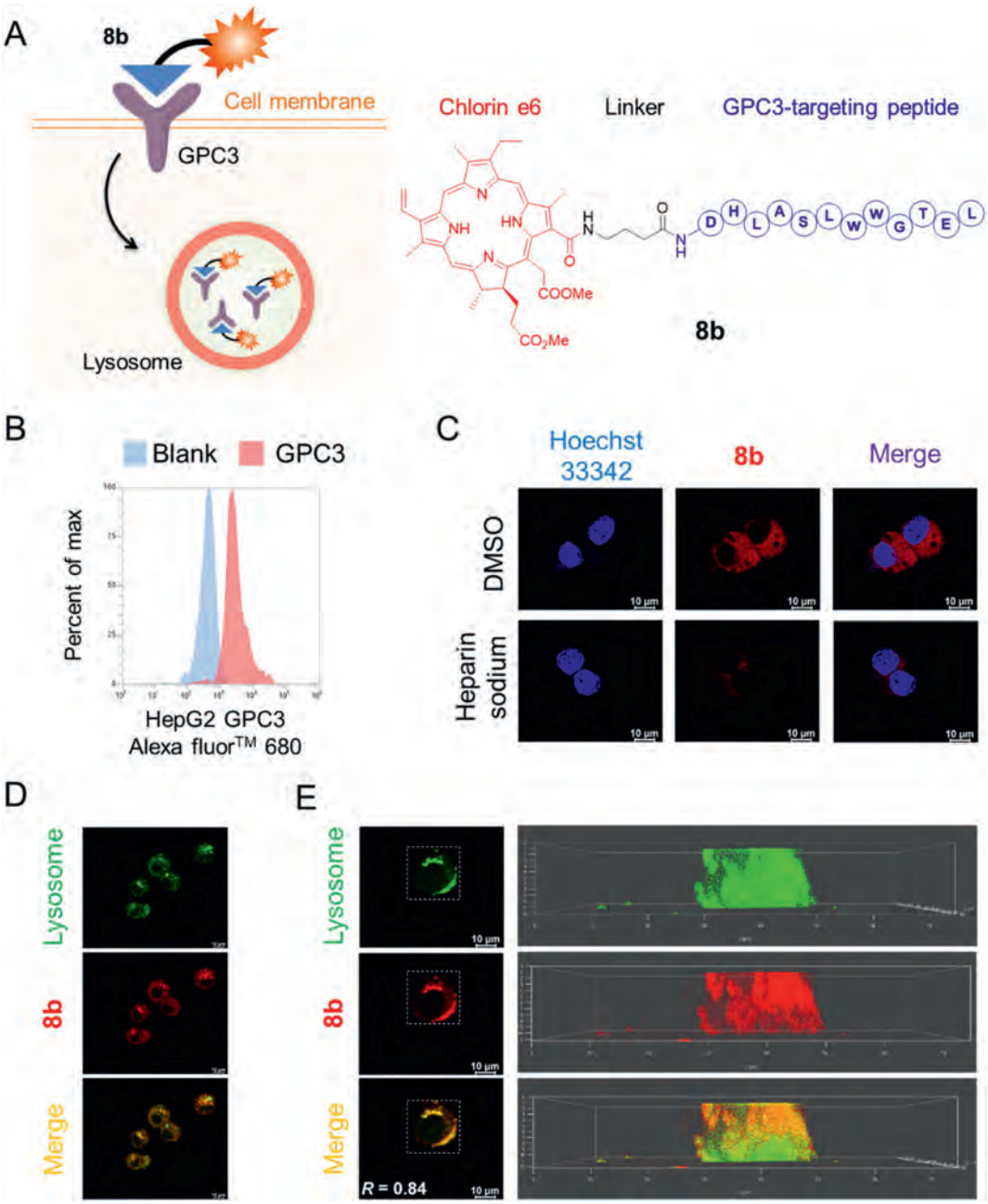

Figure 2 GPC3-mediated endocytosis and lysosomal trafficking using a probe conjugating GPC3-targeting peptide with photosensitizer. (A) Schematic diagram of the internalization of probe **8b** mediated by GPC3. (B) GPC3 protein expression level in HepG2 cells. (C) Cellular uptake of probe **8b** (2 μmol/L) in HepG2 cells using confocal laser scanning. (D) Colocalization of probe **8b** (red) with the lysosome marker (green) in HepG2 cells. (E) Colocalization of probe **8b** (red) with the lysosome marker (green) by 3D fluorescence confocal assay. Pearson coefficient $R = 0.84$. For Fig. 2C–E, Scale bar = 10 μm.

quantification of cell-surface PD-L1 was assessed by confocal microscopy. PD-L1 protein was labeled with a fluorescence antibody. After treatment with **WP0**, a significant reduction in the fluorescence intensity of the cell membrane was observed (Fig. 3B), confirming the elimination of PD-L1 on the cell surface. These results were consistent with the findings from the Western blot assays.

To evaluate the universality of the GLTAC degradation strategy in different cell lines, human colon cancer Caco-2 cells that simultaneously express GPC3 and PD-L1 (Fig. 3C) were selected for the degradation activity test. Western blot analysis showed that GLTACs **WP0** and **WP1** also exhibited PD-L1 degradation activities in Caco-2 cells (Fig. 3D, Supporting Information Fig. S11), and the SAR was consistent with the observations in HepG2 cells. Specifically, compound **WP0** exhibited the best degradation activity, with a DC_{50} value of 0.55 μmol/L in Caco-2 cells (Fig. 3D, Supporting Information Fig. S5). The above results indicate that GLTACs induce efficient PD-L1 degradation in tumor cells with high GPC3 expression.

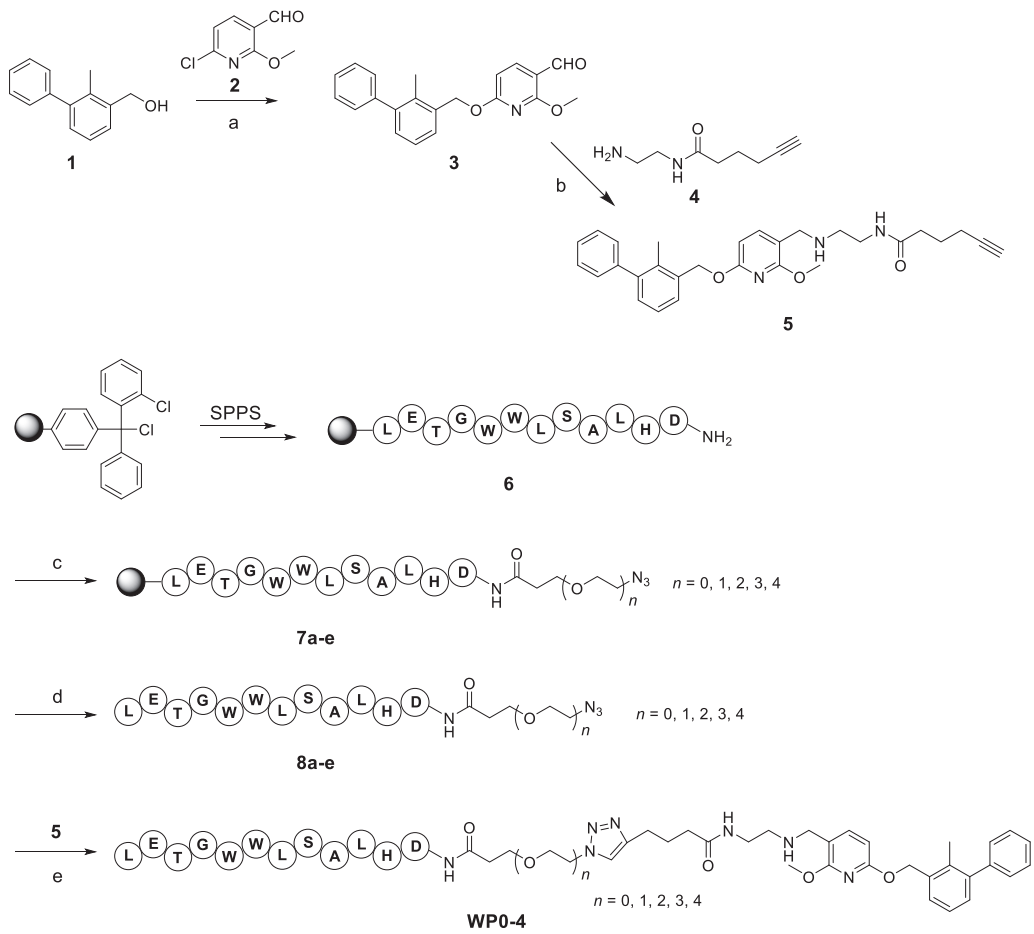

Scheme 1 Synthetic route of target compounds **WP0-4**. Reagents and conditions: (a) Cs_2CO_3, *t*-BuXPhos, $Pd(OAc)_2$, toluene, 90 °C, 1 h, 92%; (b) DIPEA, DCM, STAB, rt, 4 h, 68%; (c) azido-PEG_n-acid (n = 0, 1, 2, 3, 4), HATU, DIPEA, DMF, rt, 1 h; (d) TFA, TIPS, H_2O, rt, 1 h; (e) sodium ascorbate, $CuSO_4$, rt, 2 h, 25%−37%.

*2.4. Mechanisms of PD-L1 degradation induced by GLTAC **WP0***

GLTAC **WP0** degraded PD-L1 in a time-dependent manner in HepG2 cells (Fig. 4A, Supporting Information Fig. S12). Compound **WP0** showed degradation activity after 8 h of treatment with HepG2 cells and reached the maximum degradation at 24 h. Subsequently, we pretreated HepG2 cells with compounds **BMS-202** and **TJ12P1**, which bound to cell surface PD-L1 and GPC3, respectively, followed by the addition of **WP0** for co-incubation. The results revealed that pretreatment with **BMS-202** or **TJ12P1** blocked the PD-L1 degradation induced by compound **WP0** in HepG2 cells (Fig. 4B, Supporting Information Fig. S13). To further verify the degradation mechanism of compound **WP0**, HepG2 cells were pretreated with **MG132** (a proteasome inhibitor) or **bafilomycin A** (**BafA**, a lysosome inhibitor) before co-incubation with compound **WP0**. Only lysosome inhibitor **BafA** reversed the PD-L1 degradation induced by compound **WP0**, indicating that GLTAC **WP0** exerted the PD-L1 degradation effect through the lysosomal pathway (Fig. 4B). To investigate the importance of GPC3 in the GLTAC strategy, MDA-MB-231 cells that expressed PD-L1 but not GPC3 (Fig. 4C) were used to assess the degradation activity. As expected, GLTAC **WP0** failed to show PD-L1 degradation activity (Fig. 4D, Supporting Information Fig. S14), indicating that the degradation activity of GLTAC **WP0** was dependent on GPC3. In addition, quantitative real-time PCR experiments were conducted to detect whether the mRNA level of PD-L1 changed upon **WP0** treatment. As shown in Supporting Information Fig. S6, **WP0** did not affect the mRNA levels of PD-L1 in HepG2 cells.

To investigate the mechanism of action of GLTAC **WP0** with GPC3 and PD-L1, a cellular thermal shift assay (CETSA) was utilized to evaluate the binding ability of **WP0** with the two target proteins. The results demonstrated that compound **WP0** exhibited significant thermal stabilization effects on both PD-L1 and GPC3 (Fig. 5A, Supporting Information Fig. S15), confirming the binding ability of compound **WP0** with both proteins in HepG2 cells. Microscale thermophoresis (MST) assay was then performed to determine the binding affinities of compound **WP0** with the two target proteins. The K_D values were determined to be 348 nmol/L and 11 μmol/L with GPC3 and PD-L1 (Fig. 5B), respectively, which were comparable to those of **TJ12P1** and **BMS-202** (Supporting Information Fig. S7).

The ability of the LYTAC-like bifunctional molecule to induce the formation of a ternary complex between the lysosomal-targeting receptor and POI is crucial for the degradation process. Therefore, the formation of a ternary complex between GLTAC, GPC3, and PD-L1 is essential for PD-L1 degradation. Using fluorescence antibodies to label PD-L1 and GPC3 in HepG2 cells, the spatial distribution of these proteins was examined by

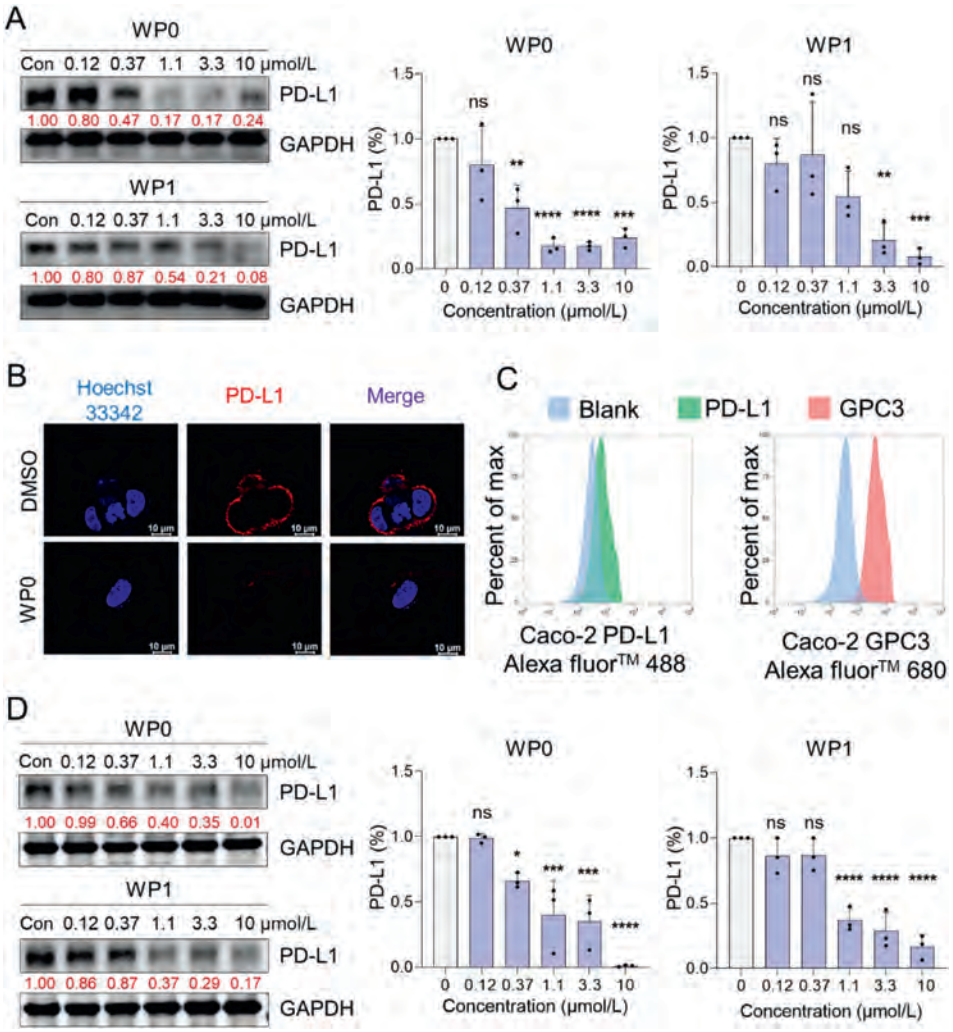

Figure 3 PD-L1 degradation activities of GLTACs. (A) PD-L1 degradation activity of compounds **WP0** and **WP1** in HepG2 cells. Data are presented as mean ± SD ($n = 3$). $^{**}P < 0.01$, $^{***}P < 0.001$, $^{****}P < 0.0001$, ns, not significant. (B) Representative confocal micrographs of the PD-L1 degradation activity of compound **WP0** (3 μmol/L) in HepG2 cells. Scale bar = 10 μm. (C) GPC3 and PD-L1 protein expression levels in Caco2 cells. (D) PD-L1 degradation activity of compounds **WP0** and **WP1** in Caco2 cells. Data are presented as mean ± SD ($n = 3$). $^{*}P < 0.1$, $^{***}P < 0.001$, $^{****}P < 0.0001$, ns, not significant. Uncropped blot images for Fig. 3A and D are shown in Supporting Information Figs. S10 and S11. The red numbers in Fig. 3A and D represent the percentage of PD-L1 remaining relative to the control.

fluorescence confocal microscopy. In the control group, the colocalization of PD-L1 and GPC3 in HepG2 cells was low, with a Pearson coefficient of only 0.21. After the treatment with GLTAC **WP0**, the colocalization of PD-L1 and GPC3 significantly increased with a Pearson coefficient of 0.80 (Fig. 5C), suggesting that GLTAC **WP0** induced the aggregation and colocalization of PD-L1 and GPC3. To directly verify the formation of the ternary complex, cell lysates from HepG2 cells were incubated with GLTAC **WP0**, and Western blot analysis was conducted to detect the formation of the ternary complex. Compared to the control group, the protein band corresponding to the PD-L1-**WP0**-GPC3 ternary complex was observed in the **WP0**-treated group (Fig. 5D, Supporting Information Fig. S16). To further explore the binding mode of **WP0** with PD-L1 and GPC3, molecular modeling was performed to understand the structural details of the PD-L1-**WP0**-GPC3 ternary complex[29]. As shown in Supporting Information Fig. S8, both ligands of **WP0** occupied the binding pockets of PD-L1 and GPC3, respectively, suggesting favorable conditions for the formation of a ternary complex with a suitable length of linker. These results confirm that GLTAC **WP0** can induce the aggregation and colocalization of PD-L1 with GPC3 in cells, forming the PD-L1-**WP0**-GPC3 ternary complex, which then undergoes internalization into lysosomes for degradation.

2.5. GLTAC WP0 induced T-cell-mediated tumor killing against HepG2 cells

To evaluate the ability of GLTAC **WP0** to kill tumor cells in the presence of T cells, we detected the T-cell-mediated tumor cell killing in a co-culture system of tumor cells and Jurkat T cells. The testing compounds were added to HepG2 cells for 24 h before co-incubation with Jurkat cells to simulate the effector T lymphocyte recognition and killing of tumor cells, and the cell viability of HepG2 cells was measured using a CCK-8 assay (Fig. 6A). The results demonstrated that both PD-L1 degrader **WP0** and inhibitor **BMS-202** effectively induced Jurkat T-cell-mediated cytotoxicity against HepG2 cells (Fig. 6B). Traditional PD-L1 small molecule inhibitors often limited by off-target effects and toxicities to

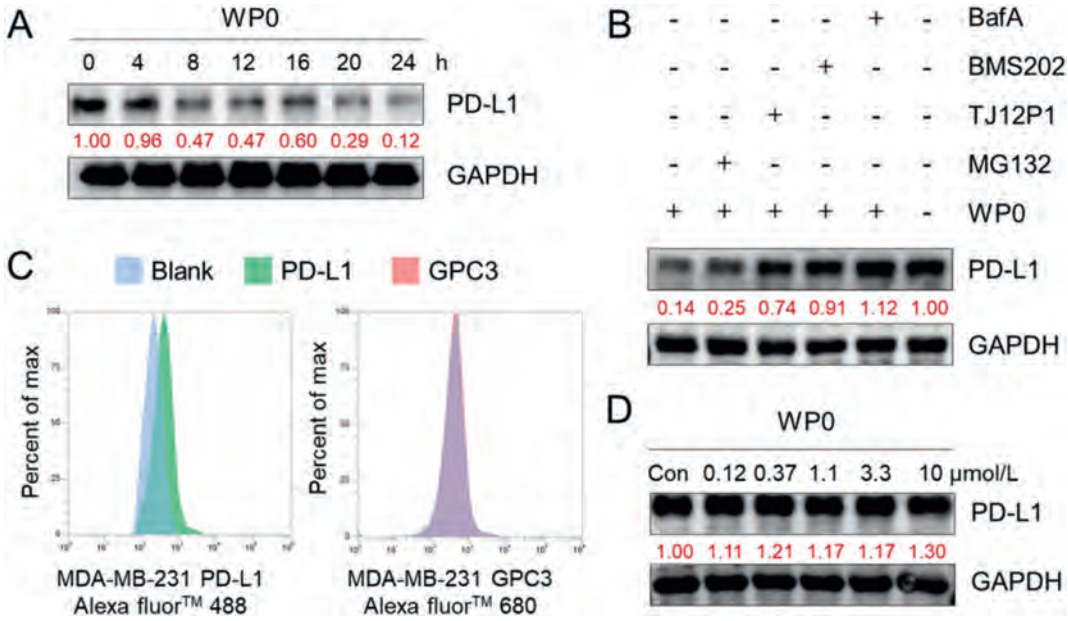

Figure 4 Degradation mechanisms of PD-L1 GLTAC. (A) Time-dependent degradation activity of compound **WP0** (3 μmol/L) in HepG2 cells. (B) PD-L1 protein level in HepG2 cells. Cells were pretreated with lysosome inhibitor **BafA** (100 nmol/L), **BMS-202** (1 μmol/L), **TJ12P1** (1 μmol/L), or proteasome inhibitor **MG132** (100 nmol/L), followed by treatment with **WP0** (1 μmol/L). (C) GPC3 and PD-L1 protein expression levels in MDA-MB-231 cells. (D) Degradation activity of **WP0** on PD-L1 protein in MDA-MB-231 cells. Uncropped blot images for Fig. 4A, B and D are shown in Supporting Information Figs. S12−S14. The red numbers in Fig. 4A, B and D represent the percentage of PD-L1 remaining relative to the control.

normal cells[33]. Therefore, the toxicity of compounds **WP0** and **BMS-202** was evaluated against L02 normal cells lacking expression of PD-L1 and GPC3 (Supporting Information Fig. S9). As shown in Fig. 6C, PD-L1 inhibitor **BMS-202** showed obvious cytotoxicity at a concentration of 10 μmol/L, leading to significant L02 cell death. In contrast, GLTAC **WP0** at the same concentration did not exhibit cytotoxicity. These findings indicate that GLTAC **WP0** effectively induces PD-L1 degradation, resulting in selective Jurkat T-cell-mediated cytotoxicity against HepG2 cells. The mechanism of action of GLTAC relies on the interaction between the GPC3-targeting peptide and the GPC3 receptor to achieve the targeted degradation effect. Since normal cells, such as L02, do not express GPC3, GLTAC **WP0** cannot be internalized by these cells *via* GPC3-mediated endocytosis, thus minimizing the cytotoxicity that might arise from off-target effects. This selective targeting and degradation pathway highlights the potential of GLTAC technology for developing precision cancer therapy with reduced side effects.

2.6. Exploring the target scope of GLTAC technology

To validate the target scope of GLTAC technology, we selected membrane proteins c-Met and FGFR1 to design GLTAC degraders. Aberrant activation of c-Met is closely associated with the development of HCC[34], making it a promising target for the clinical treatment of HCC. Tyrosine kinase receptor FGFR1 is highly expressed in various tumors including liver cancer, which serves as a tumor marker and a target for cancer therapy[35]. The GLTAC strategy we developed relies on bifunctional molecules that bind simultaneously to the GPC3 protein and the target protein outside the cell membrane. Therefore, peptides that bind to the extracellular domains of c-Met and FGFR1 were chosen for the development of lysosome-targeting chimeras. Utilizing the GLTAC technology, we conjugated GPC3-targeting peptide with c-Met-binding peptide (DQIIANN)[36] and FGFR1-binding peptide (KAEWKSLGEEAWHSK)[37] through click reaction to obtain c-Met GLTAC **GCM** and FGFR1 GLTAC **GFG**, respectively (Fig. 7A, Supporting Information Schemes S2 and S3). Western blot assay demonstrated that **GCM** and **GFG** concentration-dependently degraded c-Met and FGFR1 in both HepG2 and Caco-2 cells (Fig. 7B and C, Supporting Information Figs. S17 and S18). Fluorescence confocal experiments showed that **GCM** and **GFG** could significantly downregulate c-Met and FGFR1 at the cell membrane *in situ* (Fig. 7D−G). These findings confirm that GLTAC may have a broad target scope and is applicable to more membrane proteins.

3. Conclusions

The development of TPD technologies, particularly for extracellular and membrane proteins, represents a significant advancement in the field of drug discovery and chemical biology. In this study, we developed GLTAC as a novel lysosome-targeting strategy for the targeted degradation of tumor-specific membrane proteins. Leveraging the tumor-specific expression and endocytosis properties of GPC3, GLTACs enable the selective internalization and degradation of key membrane proteins in cancer cells. As a proof-of-concept study, GLTAC degraders targeting PD-L1, c-Met, and FGFR1 were designed. These compounds demonstrated remarkable degrading efficacy in tumor cells. Particularly, GLTAC **WP0** showed a DC_{50} value of 0.38 and 0.55 μmol/L for PD-L1 degradation in HepG2 cells and Caco-2 cells, respectively. The degradation activity was confirmed to be dependent on GPC3 expression and lysosomal pathway.

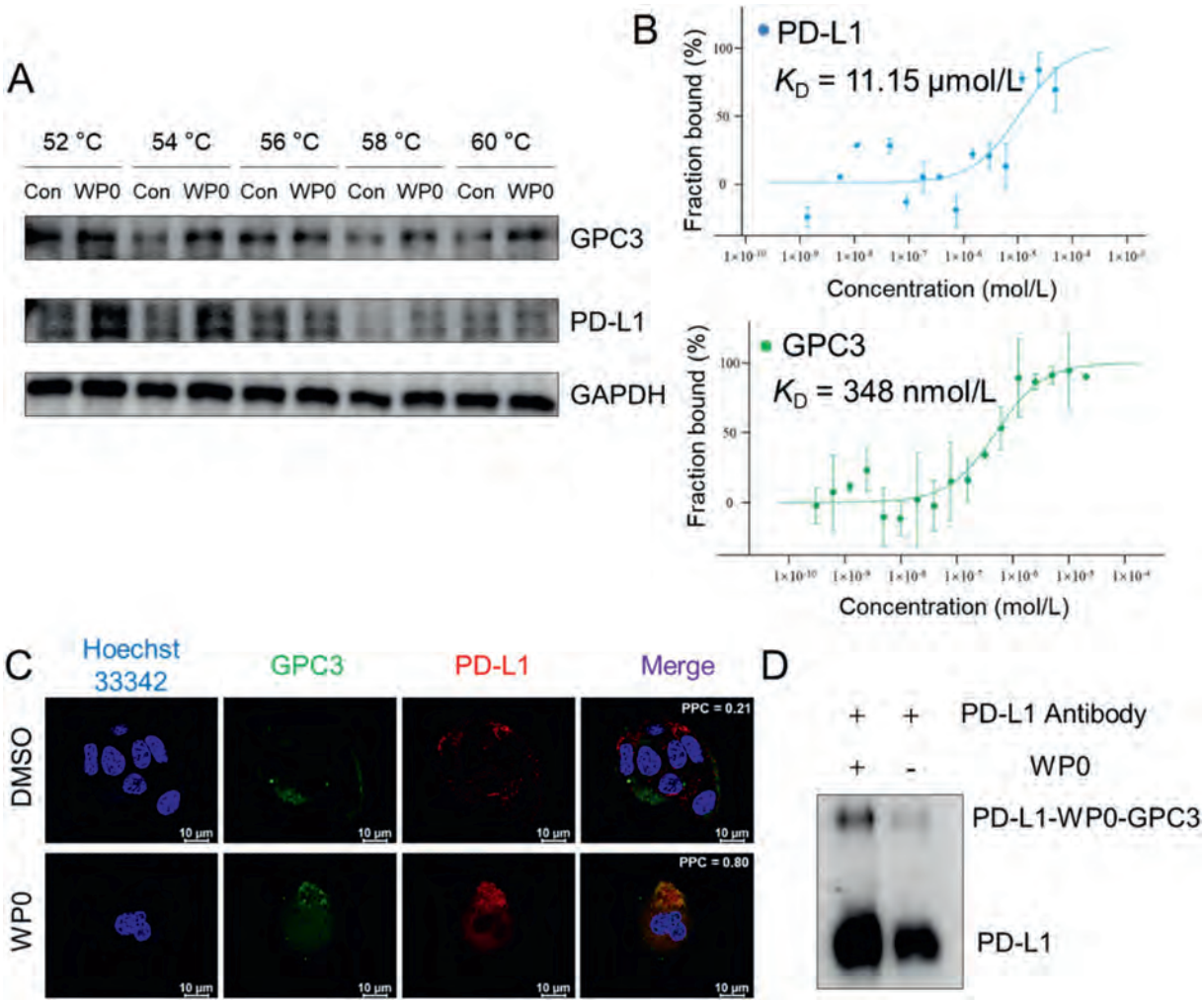

Figure 5 Binding of GLTAC **WP0** with GPC3 and PD-L1 and the formation of ternary complex. (A) Binding of compound **WP0** (5 μmol/L) with GPC3 and PD-L1 verified by CETSA. (B) Binding affinity of compound **WP0** with GPC3 and PD-L1 measured by MST assay. Data were represented as mean ± SD (n = 3). (C) Colocalization of GPC3 and PD-L1 induced by compound **WP0** (3 μmol/L) by confocal microscopy. Scale bar = 10 μm. (D) Compound **WP0** (5 μmol/L) induced the PD-L1-**WP0**-GPC3 ternary complex formation. Uncropped blot images for Fig. 5A and D are shown in Supporting Information Figs. S15 and S16.

The mechanism of action of GLTACs involves the formation of a ternary complex between GPC3, the GLTAC molecule, and the POI, leading to internalization and degradation in lysosomes. Confocal microscopy and Western blot assays confirmed the aggregation and colocalization of POIs with GPC3 in the presence of GLTACs. The target scope of the GLTAC strategy was further extended to c-Met and FGFR1 in different cell lines. These results highlight the versatility and potential of GLTAC technology in addressing the challenges of membrane protein degradation. In particular, GLTAC **WP0** potently induced T-cell-mediated tumor killing against HepG2 cells without cytotoxicity to normal cells, highlighting the superior therapeutic potential. However, the protein degradation activity of **WP0** needs to be enhanced, and the *in vivo* antitumor efficacy of GLTACs requires further investigation.

In summary, this study highlights GLTACs as a promising new approach for targeted degradation of tumor-specific membrane proteins. GLTAC has the advantages of high specificity and efficacy, rational molecular design, and convenient synthesis, which offers a valuable tool to the arsenal of TPD strategies and holds the promise to degrade challenging protein targets. Further exploration of the therapeutic effects of GLTACs in precision cancer therapy is expected to expand the scope of TPD.

4. Materials and methods

4.1. Chemistry

4.1.1. General methods

^{1}H NMR and ^{13}C NMR spectra were recorded on Bruker AVANCE II 300 or AVANCE II 600 spectrometer (Bruker, AVANCE II 300 or AVANCE II 600, Baden-Württemberg, Germany), using TMS as an internal standard and DMSO-d_6 as solvents (Energy Chemical, EG9002, Anhui, China). Chemical shifts (δ values) and coupling constants (J values) are given in ppm and Hz, respectively. The High-resolution Mass Spectrometry (HRMS) spectra were recorded on mass spectrometers (Agilent, 1260UPLC-6500 Q-TOF MS, CA, USA) (SHIMADZU, LCMS-8040, Kyoto Prefecture, Japan). Silica gel thin-layer

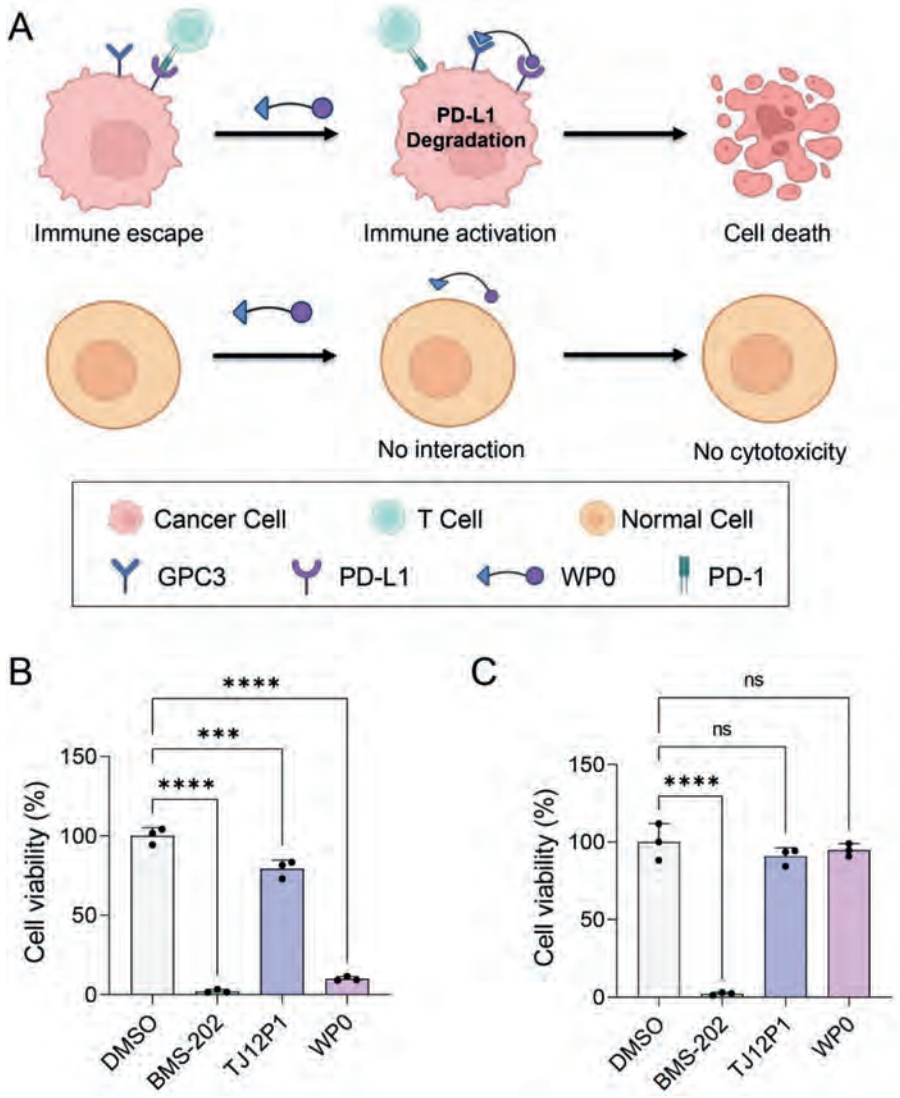

Figure 6 Cellular effect of GLTAC **WP0** in cancer immunotherapy. (A) Schematic diagram of the action mode of compound **WP0**. Fig. 6A was created with BioRender.com. (B) Effects of compounds **WP0** and **BMS-202** to induce T-cell-mediated tumor killing against HepG2 Cells. (C) Cytotoxic effect of compound **WP0** and **BMS-202** on normal L02 cells. Data were represented as mean ± SD ($n = 3$). ***$P < 0.001$, ****$P < 0.0001$, ns, not significant.

chromatography was performed on precoated plates GF-254 (Titan, Cat. No. 02156237, Shanghai, China). Silica gel column chromatography was performed with Silica Flash (Titan, Cat. No. 02151220, Shanghai, China). The purity of the compound was analyzed by High-Performance Liquid Chromatography (SHIMADZU, SIL-20AXR, Kyoto Prefecture, Japan), and the final compounds exhibited a purity greater than 95%. The applied mobile phases were 90% CH_3CN/10% H_2O. Flow speed was 1.0 mL/min and injection volumes were 5 μL or 50 μL.

4.1.2. Materials

1-Ethyl-3-(3-dimethylaminopropyl)carbodiimide (EDCI), 1-hydroxybenzotriazole (HOBT), *N*,*N*-di-*iso*-propylethylamine (DIPEA), dichloromethane (DCM), 6-chloro-2-methoxyni-cotinaldehyde, Cs_2CO_3, 2-di-tert-butylphosphino-2′,4′,6′-trisopropylbinphenyl, *N*,*N*′-di-*iso*-propylcarbodiimide (DIC), $Pd(OAc)_2$, toluene, sodium triacetoxyborohydride (STAB), *N*,*N*-dimethylformamide (DMF), Fmoc-amino acids, 1-[*bis*-(dimethylamino)-methylene]-1*H*-1,2,3-triazolo[4,5-*b*]-pyridinium 3-oxid hexafluorophosphate (HATU), trifluoroacetic acid (TFA), 4-pentynoic acid, tri-*iso*-propylsilane (TIPS), $CuSO_4$ and sodium ascorbate were purchased from Bide Pharmatech Co., Ltd., J&K Co., Ltd. and Titan Co., Ltd.

4.1.3. Synthesis procedures

*4.1.3.1. Synthesis procedure of 2-methoxy-6-((2-methyl-[1,1′-biphenyl]-3-yl) methoxy) nicotinaldehyde (**3**).* Compound **1** (0.50 g, 2.52 mmol/L), 6-chloro-2-methoxynicotinaldehyde (**2**) (0.44 g, 2.52 mmol/L), Cs_2CO_3 (1.6 g, 5.04 mmol/L), 2-di-*tert*-butylphosphino-2′,4′,6′-trisopropylbinphenyl (0.22 g, 0.50 mmol/L), $Pd(OAc)_2$ (42 mg, 0.252 mmol/L) were dissolved in toluene (25 mL). The mixture was stirred for 1 h at 90 °C. After completion of the reaction, the mixture was filtered and the solvent was removed under the reduced pressure. The crude product was purified by column chromatography (PE/EA = 10:1) to give intermediate **3** as a white solid (772 mg, yield 92%). ^{1}H NMR (300 MHz, DMSO-d_6) δ: 10.09 (s, 1H), 8.03 (d, $J = 8.3$ Hz, 1H), 7.50−7.18 (m, 8H), 6.59

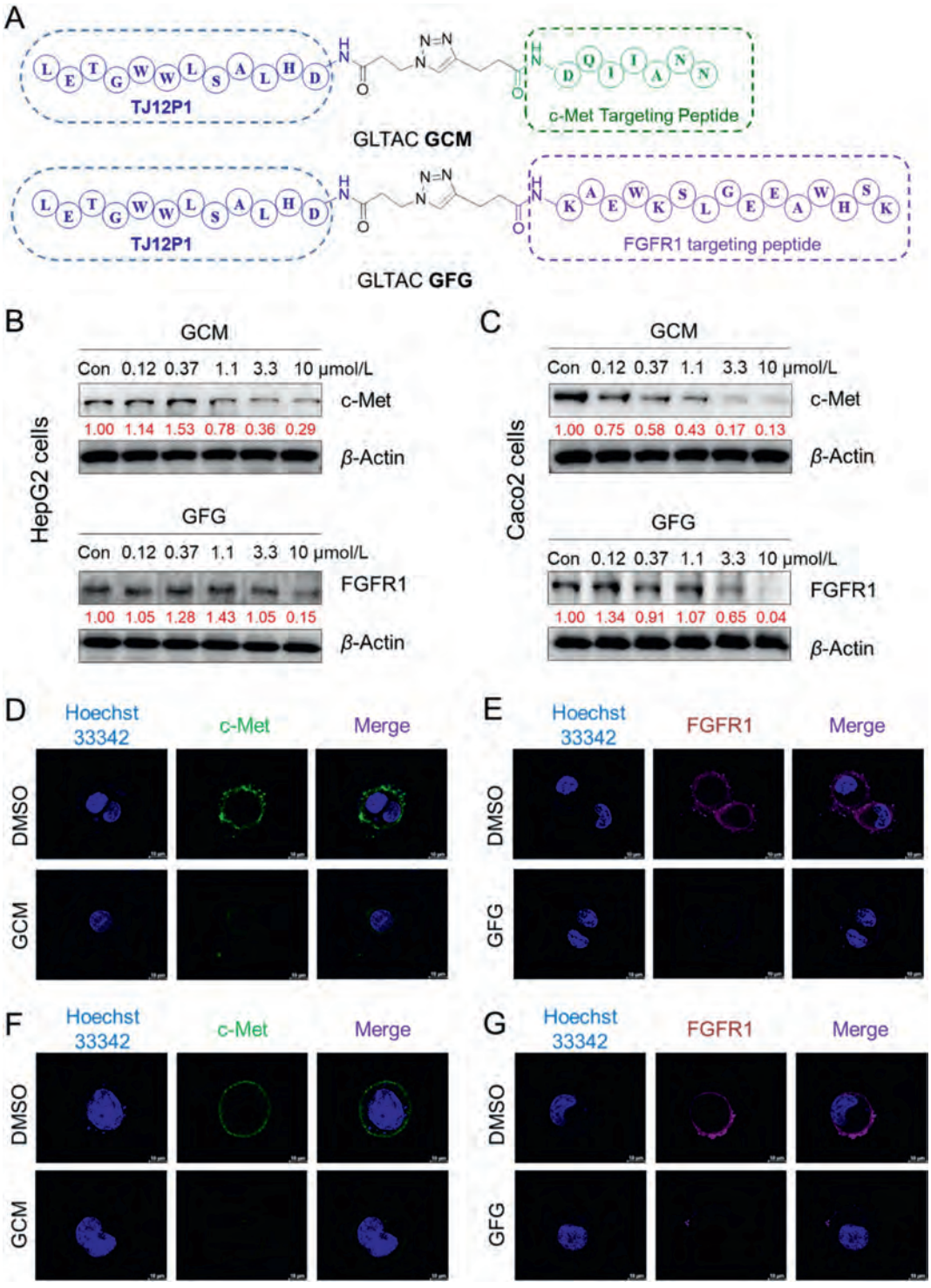

Figure 7 Validation of the target scope of the GLTAC strategy. (A) The chemical structures of **GCM** (a c-Met degrader) and **GFG** (a FGFR1 degrader). (B) Degradation activity of **GCM** and **GFG** in HepG2 cells. (C) Degradation activity of **GCM** and **GFG** in Caco2 cells. (D) Representative confocal micrographs of the c-Met degradation activity of **GCM** (5 μmol/L) in HepG2 cells. (E) Representative confocal micrographs of the FGFR1 degradation activity of **GFG** (5 μmol/L) in HepG2 cells. (F) Representative confocal micrographs of the c-Met degradation activity of **GCM** (5 μmol/L) in Caco2 cells. (G) Representative confocal micrographs of the FGFR1 degradation activity of **GFG** (5 μmol/L) in Caco2 cells. For Fig. 7D−G, Scale bar = 10 μm. Uncropped blot images for Fig. 7B and C are shown in Supporting Information Figs. S17 and S18. The red numbers in Fig. 7B and C represent the percentage of target proteins remaining relative to the control.

(d, J = 8.3 Hz, 1H), 5.55 (s, 2H), 4.04 (s, 3H), 2.22 (s, 3H). ^{13}C NMR (75 MHz, DMSO-d_6) δ: 186.6, 165.8, 164.2, 142.2, 141.2, 140.6, 134.9, 134.0, 129.8, 129.1, 128.5, 128.2, 126.9, 125.5, 111.8, 103.5, 67.2, 53.9, 15.9. HRMS (ESI) *m/z*: Calcd. for $C_{21}H_{19}NO_3$ $[M + H]^+$ 334.1438, Found: 334.1431.

*4.1.3.2. Synthesis procedure of N-(2-(((2-methoxy-6-((2-methyl-[1,1′-biphenyl]-3-yl) methoxy) pyridin-3-yl) methyl) amino) ethyl) hex-5-ynamide (**5**).* The intermediate **S3** (1.10 g, 4.33 mmol/L) was poured into 4 mol/L HCl in dioxane. The reaction mixture was stirred at room temperature overnight. Then, the reaction mixture was evaporated under reduced pressure, and the crude product (**4**) was dissolved in DCM (30 mL) with DIPEA (0.87 mL, 5.00 mmol/L). Then, add STAB (1.69 g, 7.99 mmol/L) and intermediate **3** into the mixture, stirred for 4 h at room temperature. After completion of the reaction, the mixture was washed with water and evaporated under reduced pressure. The crude product was purified by column chromatography (MeOH/DCM = 1:25) to give compound **5** as a yellow oil (1.66 g, yield 68%). ^{1}H NMR (600 MHz, DMSO-d_6) δ: 7.91 (t, J = 5.5 Hz, 1H), 7.67 (d, J = 8.0 Hz, 1H), 7.46−7.42 (m, 3H), 7.40−7.35 (m, 1H), 7.32−7.28 (m, 2H), 7.26 (t, J = 7.6 Hz, 1H), 7.18 (dd, J = 7.6, 1.2 Hz, 1H), 6.44 (d, J = 7.9 Hz, 1H), 5.75 (s, 1H), 5.41 (s, 2H), 3.90 (s, 3H), 3.68 (s, 2H), 3.21−3.17 (m, 2H), 2.78 (t, J = 2.6 Hz, 1H), 2.62 (t, J = 6.4 Hz, 2H), 2.21 (s, 3H), 2.18−2.12 (m, 4H), 1.65 (m, 2H). ^{13}C NMR (150 MHz, DMSO-d_6) δ: 171.6, 161.0, 159.8, 142.1, 141.7, 141.4, 135.9, 133.8, 129.5, 129.1, 128.2, 126.9, 125.4, 111.6, 100.8, 84.0, 71.4, 66.2, 53.2, 48.5, 47.5, 45.5, 37.7, 34.1, 24.2, 17.3, 15.9. HRMS (ESI) *m/z*: Calcd. for $C_{29}H_{33}N_3O_3$ $[M + H]^+$ 472.2595, Found: 472.2584, $[M + Na]^+$ 494.2414, Found: 494.2411.

4.2. Cell culture

HepG2, Caco2, MDA-MB-231, and L02 cells used in the experiment were purchased from the National Collection of Authenticated Cell Cultures (Shanghai, China). HepG2 and Caco2 cells were cultured using MEM containing NEAA as the basic culture medium (Pricella Life Science & Technology Co., Ltd., Cat No. PM150410, Wuhan, China). MDA-MB-231 and L02 cells were cultured using DMEM as the basic culture medium (Pricella Life Science & Technology Co., Ltd., Cat No. PM150210). All cells were added with 10% FBS (Pricella Life Science & Technology Co., Ltd., Cat No. 164210-50), 1% penicillin-streptomycin solution (Pricella Life Science & Technology Co., Ltd., Cat No. PB180120) and cultured at 37 °C, 5% CO_2.

4.3. Measurement of membrane protein expression

HepG2, Caco2, MDA-MB-231, and L02 cells were cultured using the corresponding culture media. Cells were digested and collected when they were in the logarithmic growth phase. Then, washed with PBS (Pricella Life Science & Technology Co., Ltd., Cat No. PB180327) 3 times and resuspended in Normal Donkey Serum (Solarbio, Cat No. SL050, Beijing, China)-PBS solution (10%, 2 mL) at 37 °C, 5% CO_2 for 30 min. Cells were centrifuged and collected. PD-L1 monoclonal antibody (Proteintech, Cat No. 66248-1-Ig, Wuhan, China) (1:200, 1 mL) or Glypican 3 polyclonal antibody (Proteintech, Cat No. 25175-1-AP) (1:200, 1 mL) was added and incubated at 37 °C, 5% CO_2 for 1 h. After washing with PBS for 3 times, Goat Anti-Mouse IgG H&L (Alexa Fluor® 488) (Abcam, Cat No. ab150113, Cambridge, Britain) (1:200, 1 mL) was added to label the PD-L1 monoclonal antibody, Goat Anti-Rabbit IgG H&L (Alexa Fluor® 680) (Abcam, Cat No. ab175773) (1:200, 1 mL) was added to label the Glypican 3 polyclonal antibody respectively. After incubating at 37 °C for 1 h, cells were collected and washed with PBS 3 times. The fluorescent intensity on the cell surface was detected by flow cytometry (Thermo Fisher Scientific, Attune NxT, Massachusetts, USA).

4.4. Competitive inhibition of internalization mediated by GPC3

HepG2 cells were seeded in a confocal culture dish at a density of 8×10^4 cells per well. Heparin sodium (Bide Pharmatech Co., Ltd., Cat No. BD105714, Shanghai, China) (10 μmol/L, 2 mL) was added and incubated with cells for 2 h. After washing with PBS, **8b** (2 μmol/L, 2 mL) was added and incubated for 4 h. Cells were washed with PBS and fixed with paraformaldehyde fixation solution (Yeasen, Cat No. 60536ES60, Shanghai, China) (4%, 2 mL) for 15 min. Then, Hoechst 33,342 solution (Yeasen, Cat No. 40731ES10) (1 μg/mL, 2 mL) was added and cells were stained at 37 °C for 10 min. After washing with PBS 3 times, the fluorescence was observed and photographed using a confocal microscope (Leica, SP8, Germany).

4.5. Measuring the colocalization of *8b* with lysosomes

HepG2 cells were seeded in a confocal culture dish at a density of 8×10^4 cells per well. Cells were incubated with **8b** (2 μmol/L, 2 mL) for 24 h. Then, LysoTracker Green DND-26 (Yeasen, Cat No. 40738ES50) (50 nmol/L, 2 mL) was added and incubated for 5 min. After washing with PBS 3 times, the fluorescence was observed and photographed using a confocal microscope (Leica, SP8, Germany).

4.6. Western blot analysis

HepG2 and Caco2 cells were seeded in 6-well plates at a density of 3×10^5 cells per well and incubated at 37 °C, 5% CO_2 for 24 h. Compounds were diluted from 10 mmol/L stock solution to 10.00, 3.33, 1.11, 0.37, and 0.12 μmol/L in the corresponding culture media to perform concentration-dependent degradation activity test. Diluted compounds (2 mL) were added to each well of the 6-well plate and incubated for 24 h. The compound-free culture medium (2 mL) was used as a control. To perform the time-dependent degradation activity test, compounds were diluted to 3 μmol/L and added to each well of the 6-well plate at 0, 4, 8, 12, 16, and 20 h, respectively. After incubating compounds with cells for the specified time, the original culture medium was discarded and cells were washed with pre-cooled PBS 3 times. RIPA lysis buffer (Epizyme, Cat No. PC101, Shanghai, China) containing protease inhibitors (Epizyme, Cat No. GRF101) and phosphatase inhibitors (Epizyme, Cat No. GRF102) was added and incubated for 15 min. Cells were collected in centrifuge tubes, vortexed every 5 min for 3 times, and centrifuged at 4 °C and 12,000×g for 15 min. The supernatant was collected, and protein quantification was performed using an instant BCA Protein Assay Kit (Epizyme, Cat No. ZJ102). Samples were mixed with loading buffer (Epizyme, Cat No. LT101) and boiled for 5 min. Proteins were separated by 10% sodium dodecyl sulfate-polyacrylamide gel electrophoresis (SDS-PAGE) and transferred to 0.45 μm polyvinylidene difluoride membrane (PVDF) (Millipore, Cat No. IPFL00010). The membrane was blocked with Protein Free Rapid Blocking Buffer (Epizyme, Cat No. PS108P) for 1 h. Primary antibodies against target

proteins PD-L1 (ABclonal, Cat No. A19135, Wuhan, China), c-Met (Abcam, Cat No. ab216574), FGFR1 (Abcam, Cat No. ab76464), GAPDH (Abclonal, Cat No. A19056), GPC3 (Abclonal, Cat No. A11686), β-actin (Abclonal, Cat No. AC026) were added respectively and incubated overnight at 4 °C. After recovering the primary antibodies, the membrane was washed with 1 × TBST 3 times for 5 min each time. The secondary antibody (Abmart, Cat No. M21002, Shanghai, China) (1:2000) was added and incubated at room temperature for 1.5 h. The protein bands were scanned on a LI-COR Odyssey imaging system with a Light Chemiluminescence Kit (Epizyme, Cat No. SQ201).

4.7. *In situ protein degradation activity*

In situ protein degradation activity was measured following the protocol described in the literature[24]. HepG2 and Caoc2 cells were seeded in a laser confocal culture dish at a density of 8×10^4 cells per well. The cells were incubated with the target compounds (2 mL) for 24 h. After washing with PBS, cells were then fixed with paraformaldehyde (4%, 2 mL) for 10 min, blocked with Normal Donkey Serum-PBS solution (10%, 2 mL) for 30 min, and labeled with the primary antibodies (PD-L1, 1:200; c-Met, 1:200; FGFR1, 1:200) for 2 h at 37 °C. After recovering the primary antibodies, cells were washed with PBS and incubated with Goat Anti-Rabbit IgG AF 594 (Abmart, Cat No. M21014) or Goat Anti-Mouse IgG H&L (Abcam, Alexa Fluor® 488) for 1 h. The secondary antibody was recovered. After washing with PBS 3 times, the fluorescence was observed and photographed using a confocal microscope (Leica, SP8, Germany).

4.8. *Reversing the degradation activity of* ***WP0***

HepG2 cells were seeded in 6-well plates at a density of 3×10^5 cells per well and incubated at 37 °C, 5% CO_2 for 24 h. Cells were pretreated with **BMS-202** (MedChemExpress, Cat No. HY-19745, State of New Jersey, USA) (1 μmol/L), **TJ12P1** (1 μmol/L), **MG132** (Yeasen, Cat No. 52801ES08) (100 nmol/L), and **bafilomycin A** (Yeasen, Cat No. 53768ES76) (100 nmol/L) for 2 h, then treated with **WP0** (1 μmol/L) for another 24 h. The changes in protein levels in cells were subsequently investigated by using Western blot analysis.

4.9. *Cellular thermal shift assay*

Cellular thermal shift assay for compounds was performed using our established standard protocol[25]. HepG2 cells were collected and resuspended in 1000 μL PBS. Cells were then frozen and thawed in liquid nitrogen and a water bath repeatedly for 5 times. Cells were centrifuged at 12,000×*g*, 4 °C for 15 min. The supernatant was collected and added with **WP0** (5 μmol/L), incubated at 37 °C for 1 h. The compound-supernatant solution was then divided into centrifuge tubes with a volume of 70 μL, and heated at different temperatures for 3 min. The solution was mixed with loading buffer (5 × , 17.5 μL) and heated for another 5 min. Subsequently, Western blot analysis was performed to investigate the effect of the compound on protein thermal stability.

4.10. *Microscale thermophoresis assay*

The compound was diluted from 10 mmol/L stock solution to 100 μmol/L with PBS. Then, 16 concentration gradients with a two-fold dilution were set up. Each concentration gradient was added to a centrifuge tube in a volume of 20 μL. The recombinant human GPC3 protein (ABclonal, Cat No. RP00138) or PD-L1 protein (ABclonal, Cat No. RP00068) powder was diluted to a concentration of 200 nmol/L with PBS and added to the corresponding centrifuge tube. The compound−protein interaction solution was mixed well and incubated at room temperature for 30 min. The solution was aspirated by capillary, and the binding ability was determined using a microscale thermophoresis instrument (NanoTemper, NT.115, Germany).

4.11. *In vitro cytotoxicity assay*

L02 cells were seeded in 96-well plates at a density of 5×10^3 cells per well and incubated at 37 °C with 5% CO_2 for 24 h. The test compounds were diluted to 10 μmol/L and added to the 96-well plate, incubating with the cells for another 24 h. After removing the original solution, CCK8 (Yeasen, Cat No. 40203ES76) (10%, 100 μL) was added to cells and incubated at 37 °C for 1 h. The absorbance was detected using a microplate reader (Biotek, Synergy H2, USA), and the cell viability was then calculated.

4.12. *T-cell-mediated tumor cell killing assay*

This assay was performed according to the method reported in the literature[26]. HepG2 cells were seeded in 96-well plates at a density of 3×10^3 cells per well and incubated at 37 °C, 5% CO_2 for 24 h. Cells were then stimulated with IFN-γ (ABclonal, Cat No. RP01038). The test compounds were diluted to 10 μmol/L and added to the 96-well plate, incubating with the cells for another 24 h. Jurkat cells were cultured in a dish and stimulated with PMA (Bide Pharmatech Co., Ltd., Cat No. BD147799) and ionomycin (J&K, Cat No. 963386). The Jurkat cells were added to the above 96-well plate at a density of 1.5×10^4 cells per well and co-incubated with HepG2 cells for another 24 h. The viability of HepG2 cells in the co-culture system was detected using the CCK8 assay.

4.13. *Real-time quantitative PCR*

HepG2 cells were seeded in 6-well plates at a density of 3×10^5 cells per well and incubated at 37 °C, 5% CO_2 for 24 h. Cells were treated with **WP0** (3 μmol/L) for 24 h followed by digested and collected. The total RNA of the cells was isolated with the RNA isolation Kit (Vazyme, Cat No. RC113-00, Nanjing, China). cDNAs were synthesized with the corresponding cDNA Synthesis kit (Vazyme, Cat No. R312-00) under the guidance of the instructions. Real-time quantitative PCR was performed with the Taq Pro Universal SYBR qPCR Master Mix (Vazyme, Cat No. Q712-00) through the standard cycle program on a Real-Time PCR instrument (Thermo Fisher Scientific, QuantStudio™ 1, USA). The PCR primers to detect PD-L1 mRNA level (forward: 5′-AAC TAC CTC TGG CAC ATC CTC C-3′; reverse: 5′-CAT CCA TCA TTC TCC CTT TTC TT-3′), were synthesized and purified by Sangon Biotech (Shanghai, China). The PCR primers to detect GAPDH mRNA levels were purchased from Sangon Biotech (Shanghai, China).

Acknowledgments

This work was supported by the National Natural Science Foundation of China (grant 82422069 to Guoqiang Dong, 82373707 to Shipeng He, 82030105 to Chunquan Sheng, and 82273779 to

Guoqiang Dong), and the National Key Research and Development Program of China (grants 2022YFC3401500 to Chunquan Sheng). We thank the staff members of the Large-scale Protein Preparation System and the Integrated Laser Microscopy System at the National Facility for Protein Science in Shanghai (NFPS), Shanghai Advanced Research Institute, Chinese Academy of Science, China for providing technical support and assistance in data collection and analysis. We also thank the staff members of the Leica Microsystems (Shanghai) Trading Co., Ltd. for providing technical support and assistance in data collection and analysis.

Author contributions

Yuxin Fang: Writing − original draft, Data curation. Yaojin Zhu: Formal analysis, Data curation. Wei Wang: Methodology. Zhewei Xia: Methodology. Shipeng He: Writing − original draft, Supervision, Formal analysis, Conceptualization. Guoqiang Dong: Writing − review & editing, Conceptualization. Chunquan Sheng: Writing − review & editing, Supervision, Methodology, Funding acquisition, Conceptualization.

Conflicts of interest

The authors have no conflicts of interest to declare.

Appendix A. Supporting information

Supporting information to this article can be found online at https://doi.org/10.1016/j.apsb.2025.02.037.

References

1. Bekes M, Langley DR, Crews CM. PROTAC targeted protein degraders: the past is prologue. *Nat Rev Drug Discov* 2022;**21**:181−200.
2. Ding Y, Xing D, Fei YY, Lu BX. Emerging degrader technologies engaging lysosomal pathways. *Chem Soc Rev* 2022;**51**:8832−76.
3. Kim J, Byun I, Kim DY, Joh H, Kim HJ, Lee MJ. Targeted protein degradation directly engaging lysosomes or proteasomes. *Chem Soc Rev* 2024;**53**:3253−72.
4. Garber K. The PROTAC gold rush. *Nat Biotechnol* 2022;**40**:12−6.
5. Burslem GM, Crews CM. Proteolysis-targeting chimeras as therapeutics and tools for biological discovery. *Cell* 2020;**181**:102−14.
6. Clift D, McEwan WA, Labzin LI, Konieczny V, Mogessie B, James LC, et al. A method for the acute and rapid degradation of endogenous proteins. *Cell* 2017;**171**:1692−706.
7. Li ZZ, Ma SY, Zhang SX, Ma Z, Du LP, Li MY. Degradation of extracellular and membrane proteins in targeted therapy: status quo and quo vadis. *Drug Discov Today* 2023;**28**:103716.
8. Wells JA, Kumru K. Extracellular targeted protein degradation: an emerging modality for drug discovery. *Nat Rev Drug Discov* 2024;**23**:126−40.
9. Banik SM, Pedram K, Wisnovsky S, Ahn G, Riley NM, Bertozzi CR. Lysosome-targeting chimaeras for degradation of extracellular proteins. *Nature* 2020;**584**:291−7.
10. Whitmarsh-Everiss T, Laraia L. Small molecule probes for targeting autophagy. *Nat Chem Biol* 2021;**17**:653−64.
11. Zhu CH, Wang WS, Wang Y, Zhang Y, Li JB. Dendronized DNA chimeras harness scavenger receptors to degrade cell membrane proteins. *Angew Chem Int Ed Engl* 2023;**62**:e202300694.
12. Zheng JW, He WY, Li J, Feng XJ, Li YY, Cheng BH, et al. Bifunctional compounds as molecular degraders for integrin-facilitated targeted protein degradation. *J Am Chem Soc* 2022;**144**:21831−6.
13. Ahn G, Banik SM, Miller CL, Riley NM, Cochran JR, Bertozzi CR. LYTACs that engage the asialoglycoprotein receptor for targeted protein degradation. *Nat Chem Biol* 2021;**17**:937−46.
14. Miao YY, Gao QQ, Mao MH, Zhang C, Yang LQ, Yang Y, et al. Bispecific aptamer chimeras enable targeted protein degradation on cell membranes. *Angew Chem Int Ed* 2021;**60**:11267−71.
15. Zhang H, Han Y, Yang YF, Lin F, Li KX, Kong LH, et al. Covalently engineered nanobody chimeras for targeted membrane protein degradation. *J Am Chem Soc* 2021;**143**:16377−82.
16. Cotton AD, Nguyen DP, Gramespacher JA, Seiple IB, Wells JA. Development of antibody-based protacs for the degradation of the cell-surface immune checkpoint protein PD-L1. *J Am Chem Soc* 2021;**143**:593−8.
17. Thiel KW, Giangrande PH. Intracellular delivery of RNA-based therapeutics using aptamers. *Ther Deliv* 2010;**1**:849−61.
18. Christianson HC, Belting M. Heparan sulfate proteoglycan as a cell-surface endocytosis receptor. *Matrix Biol* 2014;**35**:51−5.
19. Zhou FB, Shang WT, Yu XL, Tian J. Glypican-3: a promising biomarker for hepatocellular carcinoma diagnosis and treatment. *Med Res Rev* 2018;**38**:741−67.
20. Yu M, Luo H, Fan ML, Wu XQ, Shi BZ, Di SM, et al. Development of GPC3-specific chimeric antigen receptor-engineered natural killer cells for the treatment of hepatocellular carcinoma. *Mol Ther* 2018;**26**:366−78.
21. Michalopoulos GK. Hepatostat: liver regeneration and normal liver tissue maintenance. *Hepatology* 2017;**65**:1384−92.
22. Capurro MI, Xu P, Shi W, Li FC, Jia A, Filmus J. Glypican-3 inhibits Hedgehog signaling during development by competing with patched for Hedgehog binding. *Dev Cell* 2008;**14**:700−11.
23. Fang YX, Ma HQ, Zhang XH, Zhang PF, Li Y, He SP, et al. Smart glypican-3-targeting peptide-chlorin e6 conjugates for targeted photodynamic therapy of hepatocellular carcinoma. *Eur J Med Chem* 2024;**264**:116047.
24. Miao YY, Gao QQ, Mao MH, Zhang C, Yang LQ, Yang Y, et al. Bispecific aptamer chimeras enable targeted protein degradation on cell membranes. *Angew Chem Int Ed Engl* 2021;**60**:11267−71.
25. Cheng J, Zhang J, He S, Li M, Dong G, Sheng C. Photoswitchable PROTACs for reversible and spatiotemporal regulation of NAMPT and NAD. *Angew Chem Int Ed Engl* 2024;**63**:e202315997.
26. Kim DH, Kim H, Choi YJ, Kim SY, Lee JE, Sung KJ, et al. Exosomal PD-L1 promotes tumor growth through immune escape in non-small cell lung cancer. *Exp Mol Med* 2019;**51**:1−13.
27. Sharma P, Goswami S, Raychaudhuri D, Siddiqui BA, Singh P, Nagarajan A, et al. Immune checkpoint therapy-current perspectives and future directions. *Cell* 2023;**186**:1652−69.
28. Pan CH, Yang HY, Lu Y, Hu SQ, Wu YZ, He QJ, et al. Recent advance of peptide-based molecules and nonpeptidic small-molecules modulating PD-1/PD-L1 protein-protein interaction or targeting PD-L1 protein degradation. *Eur J Med Chem* 2021;**213**:113170.
29. Zhang H, Zhang Y, Feng Z, Shuai M, Ma X, Wang S, et al. Discovery of novel proteolysis-targeting chimera molecules as degraders of programmed cell death-ligand 1 for breast cancer therapy. *J Med Chem* 2024;**67**:10589−600.
30. Cheng BB, Ren YC, Cao H, Chen JJ. Discovery of novel resorcinol diphenyl ether-based PROTAC-like molecules as dual inhibitors and degraders of PD-L1. *Eur J Med Chem* 2020;**199**:112377.
31. Wang YB, Zhou YY, Cao S, Sun Y, Dong ZQ, Li C, et al. *In vitro* and *in vivo* degradation of programmed cell death ligand 1 (PD-L1) by a proteolysis targeting chimera (PROTAC). *Bioorg Chem* 2021;**111**:104833.

32. Liu Y, Zheng MZ, Ma ZL, Zhou YR, Huo JF, Zhang WB, et al. Design, synthesis, and evaluation of PD-L1 degraders to enhance T cell killing activity against melanoma. *Chin Chem Lett* 2023;**34**:107762.
33. Cheng BB, Xiao Y, Xue MM, Cao H, Chen JJ. Recent advances in the development of PD-L1 modulators: degraders, downregulators, and covalent inhibitors. *J Med Chem* 2020;**63**:15389−98.
34. Bouattour M, Raymond E, Qin SK, Cheng AL, Stammberger U, Locatelli G, et al. Recent developments of c-Met as a therapeutic target in hepatocellular carcinoma. *Hepatology* 2018;**67**:1132−49.
35. Babina IS, Turner NC. Advances and challenges in targeting FGFR signalling in cancer. *Nat Rev Cancer* 2017;**17**:318−32.
36. Zhao MY, Wang YH, Liu Y, Zhang WC, Liu YK, Yang XM, et al. C7 peptide inhibits hepatocellular carcinoma metastasis by targeting the HGF/c-Met signaling pathway. *Cancer Biol Ther* 2019;**20**: 1430−42.
37. Chen Y, Han JY, Zhao Y, Zhao XM, Zhao MM, Zhang JM, et al. (18) F-labeled FGFR1 peptide: a new PET probe for subtype FGFR1 receptor imaging. *Front Oncol* 2023;**13**:1047080.